Direct-detection receiver for QPSK-modulated signals

Dagmawi Bekele*, Hitesh Sahoo, Deming Kong, Michael Galili, Kresten Yvind, Leif Katsuo Oxenløwe, and Jesper Mørk

DTU Electro, Department of Electrical and Photonics Engineering, Technical University of Denmark, Dk-2800, Kongens Lyngby, Denmark

**dbek@dtu.dk*

Abstract: We demonstrate a novel optical receiver for direct-detection of QPSK signals using microring-based photonic integrated circuit. The QPSK signal is converted into a PAM7 electrical signal, and demodulated without the need for a local oscillator.

1. Introduction

Quadrature amplitude modulation (QAM) formats are of great importance for long-haul optical communication links due to their high system capacity, increased spectral efficiency, and high receiver sensitivity [1,2]. Additionally, access to the optical field in digital form enables digital compensation of chromatic dispersion, polarization mode dispersion, and fiber nonlinearities [2]. These possibilities make coherent links suitable for long-haul and inter-data center communications [3]. However, the benefits of QAM modulation come at the cost of increased receiver digital signal processing complexity, and the need for a local oscillator (LO) laser [2,4]. These lead to high-cost, and power consumption of coherent systems, which may limit their application to inside data centers, where cost and simplicity are key requirements [3,5]. On the other hand, intensity modulation and direct detection schemes such as non-return-to-zero and 4-level pulse amplitude modulation (PAM4) are currently being used for intra-data center interconnects due to their relatively simple receiver circuit and low-cost [5].

In this paper, we propose and demonstrate proof-of-concept of a novel direct-detection receiver for quadrature phase shift-keying (QPSK) modulated signals. We discuss the receiver circuit structure together with system characterization including short transmission link with bit-error-ratio (BER) analysis. This technology eliminates the need for LO laser, and high-speed high-resolution analogue-to-digital converters, while keeping the modulation capacity of coherent modulation. Hence, it allows cost-effective deployment of coherent transceivers for intradatacenter applications.

2. Device structure

A schematic diagram of the proposed direct-detection receiver is shown in Fig. 1(a). The received QPSK signal is split into two branches each consisting of microring resonators side-coupled to bus waveguides. The resonance dips of the two ring resonators are aligned to the received signal spectrum so that the phase modulation is converted to intensity modulation. The outputs of the bus waveguides are detected by balanced photodiodes. The resulting photocurrent is converted into voltage and amplified using a transimpedance amplifier (TIA) before being converted to a digital signal for further signal processing. An optical microscope image of our demonstrator consisting of the fabricated photonic integrated circuit (PIC) chip packaged together with a commercial TIA on a high-speed printed circuit board (PCB) is shown in 1(b). For simplicity of implementation, two independent photodiodes are used in this design instead of balanced photodiodes. The PIC is fabricated at Advanced Micro Foundry (AMF) on silicon photonics platform. The light path in the chip for QPSK detection is highlighted by the white line from input grating couplers to the photodiodes.

3. 10 Gbd QPSK detection experiment

Continuous wave light from a tunable laser source centered around 1552 nm is modulated using a lithium niobate phase modulator with 10 Gbaud electrical PAM4 drive signal whose eyediagram is shown in Fig. 2. The polarization of the input light to the phase modulator is controlled using a polarization controller (PC). The resulting QPSK signal is amplified to compensate for coupling losses at the receiver. The constellation of the QPSK signal detected using conventional coherent receiver is shown in the inset. Here, a phase modulator is used instead of IQ modulator as required for our direct-detection receiver, and its simplicity compared to using an IQ modulator with

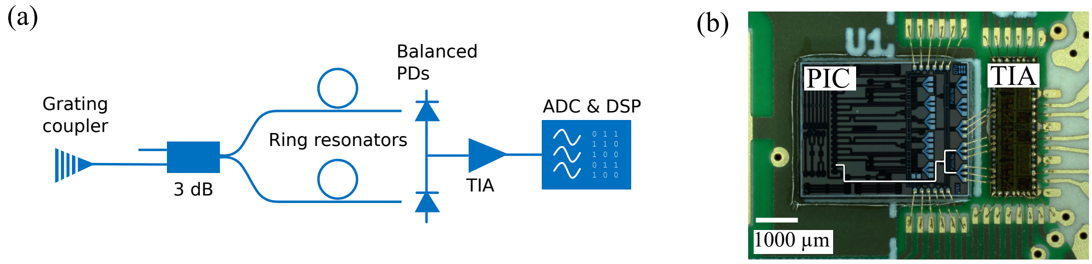

Fig. 1. (a) Schematic diagram of the proposed direct-detection receiver circuit. (b) optical microscope image of our demonstrator consisting of the photonic integrated circuit (PIC) packaged together with a TIA die on a high-speed printed circuit board.

bias controls. The constellation diagram of the QPSK signal shows slight phase noise around the four symbols of the QPSK signal. This is because during symbol transitions or phase changes in phase modulators, there is a constant power that leads to a large chirp [6]. On the other hand, when using IQ modulators for QAM modulation, the power during phase changes is low, which leads to low-chirp signal generation. After the signal is amplified, a 3 nm bandpass filter is used to remove the amplified spontaneous emission noise. The signal is then sent through a 3 km TrueWave single mode fiber with a dispersion coefficient around 2 ps/nm.km. The received signal is polarization controlled and coupled to the device under test (DUT) via grating couplers. The power of this received signal is controlled using a variable optical attenuator (VOA). Two ring resonators are used for spectral filtering of the received signal resulting in phase to intensity modulation conversion. The spectral location of the ring resonances are controlled by thermo-optic heaters. These intensity modulated signal is then detected by the photodiodes. The photocurrents from the two photodiodes are independently amplified using RF amplifiers (SHF 804). Note that for this experiment, an unpackaged PIC chip is used. The difference between these two photocurrents is determined using a 36 GHz balun. The resulting electrical signal is analyzed using either a real-time or an equivalent-time sampling oscilloscopes denoted digital storage oscilloscope (DSO), and digital communication analyzer (DCA), respectively in Fig. 2.

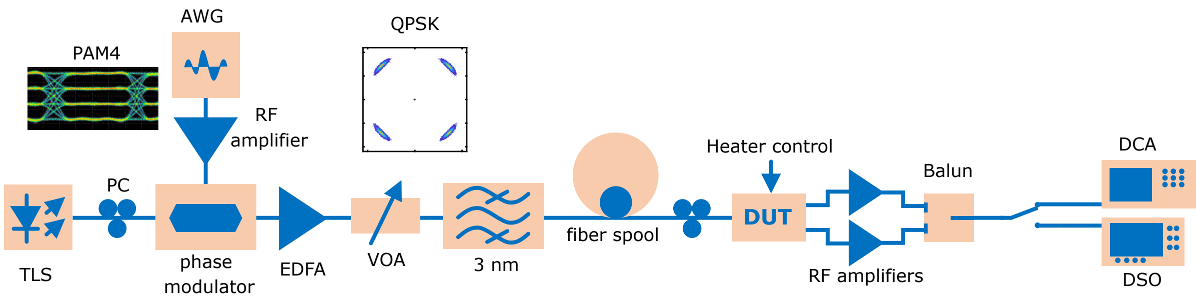

Fig. 2. Schematic diagram of the experimental setup. Light from a tunable laser source is modulated using a phase modulator with an electrical PAM4 drive signal. The resulting QPSK signal is sent to a fiber spool of 3 km before being detected by our direct detection receiver. The received signal is sampled using an 80 GSa/s real-time sampling oscilloscope.

Figure 3(a) shows the eyediagram of the PAM7 signal recorded using a DCA with 70 GHz bandwidth for back-to-back (B2B) measurement at a received optical power of 4 dBm. The lookup table in Fig. 3(b) is used to map the seven levels of the PAM7 signal to the four symbols of the transmitted QPSK signal. The amplitudes of the PAM7 signal are designated 0 to 6 starting from the lowest amplitude. The BER versus received optical power is shown in Fig. 3(c) for B2B reference measurement, and 3 km measurements. For each of the BER points, 10 million sample points were taken. A 51-Tap $T/2$-spaced feed-forward linear equalizer based on least-mean-square (LMS) algorithm is used to compensate signal impairments from the transmitter and receiver. An eyediagram of the PAM7 signal is shown in Fig. 3(d) at 4 dBm received optical power after offline equalization, and corresponds to a BER of 4×10^{-7}. The BER for B2B measurements shows a slightly lower performance than the 3 km transmission. This is due to slight drift of the heater control current resulting from unstable contacts to the heater bondpads.

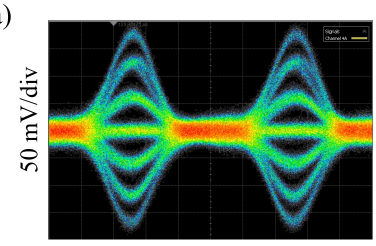

(b)

		current symbol			
		0	**1**	**2**	**3**
previous symbol	**0**	3	2	1	0
	1	4	3	2	1
	2	5	4	3	2
	3	6	5	4	3

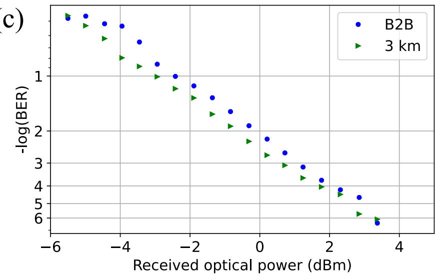

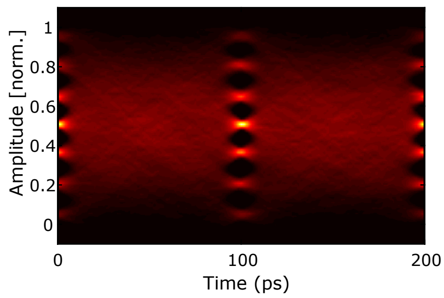

Fig. 3. (a) Measured eye-diagram of the PAM7 signal. (b) A look-up table is used to map the four symbols of QPSK to the seven levels of the PAM7 signal. (c) Bit-error ratio (BER) versus received optical power for back-to-back (B2B), and 3 km. (d) Eye-diagram of the PAM7 signal after equalization.

4. Demo content and implementation

During the demo session, a running experimental setup in the lab will be available for a remote interaction. Additionally, our proof-of-concept demonstrator PCB will be available on-site together with pre-recorded video showing the details of the setup and experiment.

5. Conclusion

We have demonstrated a direct-detection receiver circuit integrated on a silicon photonics platform. The receiver performance is evaluated using BER analysis. Current demonstration is limited to 10 Gbd due to the large half-wave voltage of our phase modulator, and quality of the electrical PAM4 drive signal. During the demo session, high-speed operation, and 16-QAM detection capabilities will be discussed.

6. Acknowledgement

The authors acknowledge financial support from Innovation Foundation Denmark, and the European Research Council via grant agreement numbers 834410 - FANO, and 101067399 - Fano Detector). Furthermore, the authors would like to thank Chip Integration Technology Center (CITC), NL for packaging our demonstrator.

References

1. A. Fallahpour, A. Mohajerin-Ariaei, A. Almaiman, Y. Cao, F. Alishahi, C. Bao, P. Liao, M. Ziyadi, B. Shamee, and D. Starodubov, "Demonstration of 30gbit/s qpsk-to-pam4 data-format and wavelength conversion to enable all-optical gateway from long-haul to datacenter," in *Optical Fiber Communication Conference*, (Optical Society of America, 2018), pp. W2A–22.
2. P. J. Winzer, D. T. Neilson, and A. R. Chraplyvy, "Fiber-optic transmission and networking: the previous 20 and the next 20 years," Opt. express **26**, 24190–24239 (2018).
3. J.-P. Elbers, N. Eiselt, A. Dochhan, D. Rafique, and H. Grießer, "PAM4 vs coherent for DCI applications," in *Signal Processing in Photonic Communications*, (Optical Society of America, 2017), pp. SpTh2D–1.
4. V. R. Pagán, B. M. Haas, and T. E. Murphy, "Linearized electrooptic microwave downconversion using phase modulation and optical filtering," Opt. express **19**, 883–895 (2011).
5. J. Cui, Y. Ji, G.-W. Lu, H. Wang, and M. Zhang, "Phase-sensitive amplifier-based optical conversion for direct detection of complex modulation format to bridge long-haul transmissions and short-reach interconnects," Opt. Express **28**, 2349–2365 (2020).
6. M. Seimetz, *High-order modulation for optical fiber transmission*, vol. 143 (Springer, 2009).